Design and Development of a 3-DOF Planar Parallel Manipulator

A thesis Submitted

in Partial Fulfillment of the Requirements

for the Degree of

Master of Technology

by

Kalva Santhosh Kumar

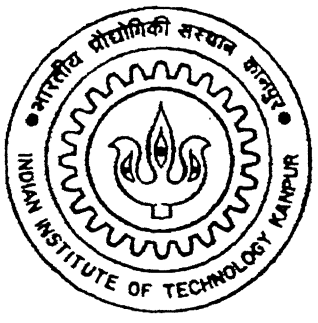

to the

DEPARTMENT OF MECHANICAL ENGINEERING

INDIAN INSTITUTE OF TECHNOLOGY, KANPUR

April, 1999

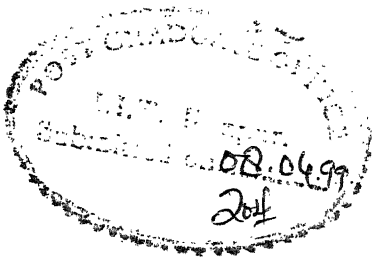

CERTIFICATE

It is certified that the work contained in the thesis entitled **Design and Development of a 3-DOF Planar Parallel Manipulator** by **Kalva Santhosh Kumar**, has been carried out under my supervision and this work has not been submitted elsewhere for a degree.

Bhaskar Dasgupta

Dr. Bhaskar Dasgupta,

Assistant Professor,

Department of Mechanical Engineering,

Indian Institute of Technology,

Kanpur. 208016.

Acknowledgement

I would like to express my deep sense of gratitude to my ever loving guide, Dr. Bhaskar Dasgupta for his invaluable guidance and constant encouragement at every step for constructive critisms and fruitful suggestions that helped me throughout the work. I am sincerely thankful to Dr. A. Mukherjee for his valuable suggestions in my work. He has been a great influence on me, both as a person and as a professional.

I am thankful to Prof. H. Hatwal for extending the facilities of the Centre for Robotics for the completion of this work. It was pleasure to be in the Centre for Robotics and I would like to thank all my colleagues and the staff at Centre for Robotics for making it a great place to work in.

I am thankful to Mr. Susmit Sen, Mrs. Anjali Kulkarni and Rajender who took great pain in developing the controller for the manipulator. I am also thankful to Mr. Jha, Mr. Namadeo, Mr. Sharma and Mr. Anil of the manufacturing lab for having helped me in the fabrication of mechanical components.

I would like to thanks my friends Duvvala, Chandu^2, Bhargava, Venu, Neeraj, Kkis, Gopal, Ranjit, Rama, Jreddy, Raju, Anil, Ganesh and all of my classmates for their help and making my stay at IIT Kanpur a pleasant and memorable one. I am thankful to my Rob. lab friends Swaroop, Nema, Vjeya and others for their help and pleasant company.

Last but not the least I would like to express my greatfulness to all those who directly or indirectly helped me through the successful completion of my work.

Kalva Santhosh Kumar.

Contents

List of Figures

List of Tables

Abstract

In this thesis, the design and development of a 3-DOF planar parallel manipulator is addressed from a kinematic viewpoint. The 3-DOF planar parallel manipulator consists of two bodies (referred to as the base and the platform) connected through three chains (two links each) having revolute joints. The workspace of this manipulator has a lot of singularities inside it where the manipulator is uncontrollable. The design should be such that it is free from singularities. The link lengths of the manipulator are calculated using optimization techniques, by keeping all singularities under considerations. Selection of materials and actuators are given. The structural design of the elements of the manipulator based on accuracy criteria is discussed. A prototype manipulator was developed as per the design. The control of actuators through interfacing the manipulator with computer is presented.

Chapter 1

Introduction

1.1 Introduction

Parallel manipulators are robotic devices that differ from the traditional serial robotic manipulators by virtue of their kinematic structure. Parallel manipulators are composed of multiple closed kinematic loops. Typically, these kinematic loops are formed by two or more kinematic chains that connect a moving platform to a base, where one joint in each chain is actuated and the other joints are passive. This kinematic structure allows parallel manipulators to be driven by actuators positioned at or near the base of the manipulator.

In contrast, serial manipulators do not have closed kinematic loops and are usually actuated at each joint along the serial linkage. Accordingly, the actuators that are located at each joint along the serial linkage can account for a significant portion of the loading experienced by the manipulator, whereas the links of a parallel manipulator generally need not carry the load of the actuators. This allows the parallel manipulator links to be made lighter than the links of an analogous serial manipulator. Hence, parallel manipulators can enjoy the potential benefits associated with light weight construction such as high-speed operation and improved load to weight ratios.

The advantage of serial manipulator is large workspace and dextrous manoeuverability like human arm, but their load carrying capacity is rather poor due to cantilever structure. Because of cantilever beam-like architecture, serial manipulators inherently suffer from some drawbacks such as low mechanical stiffness which leads to lower operational accuracy, poor dynamic characteristics and lower load carrying capacity. These disadvantages can be overcome by designing manipulators with closed kinematic loops, namely parallel manipulators.

1.2 Comparison Between Serial and Parallel Manipulators

Fig. 1.1 shows the architecture of serial and parallel manipulators. A parallel manipulator consists of two platforms connected by several legs. The top platform is usually free to move and is called the end-effector. The bottom platform is usually fixed and will be called the base. The relative positions of the end-effector and base may be reversed for some applications.

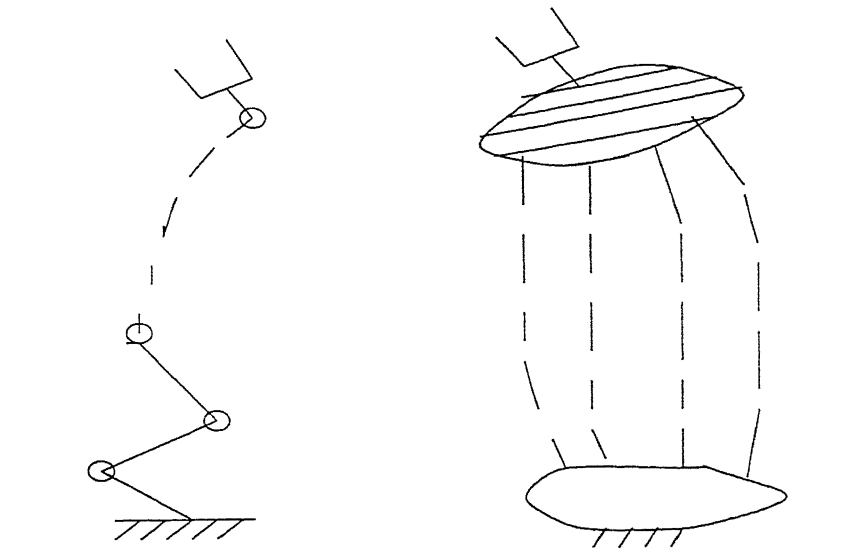

Figure 1.1: Serial and Parallel Manipulators

1.2.1 Degree of Freedom

For a serial manipulator the DOF of the system is given by

$$DOF = \sum_{i=1}^{j} f_i$$

where f_i corresponds to the DOF of the $i-$th joint of the manipulator containing j joints. In general, for serial manipulators, the DOF will be equal to the number of links as each link has a single DOF. For parallel manipulators the formula is (Grubler-Kutzbatch-Chebyshev formula)

$$DOF = n\,(L - J - 1) + \sum_{i=1}^{j} f_i$$

where L = number of links, J = number of joints, f_i = DOF of $i-$th joint and $n = 6$ for spatial manipulators while $n = 3$ for planar manipulators.

1.2.2 Direct Kinematics

The problem of direct kinematics is to find the position and orientation of the output link, given the input joint variables. The direct kinematic problem of serial manipulators turns out to be very simple by the use of Denavit-Hartenberg parameters. It can be automated for any arbitrary serial manipulator and always gives a unique solution.

In contrast, direct kinematic problem of a parallel manipulator is much more complex because of the presence of unactuated joints whose relative motions are dependent and not given. The motions of unactuated joints cannot be found from individual loops of a manipulator but from a set of simultaneous nonlinear equations involving all the loops of the manipulator. It is important to note that forward kinematics of parallel manipulator always gives multiple solutions.

1.2.3 Inverse Kinematics

The problem of inverse kinematics is to find out the required values of the input joint variables for a given position and orientation of the output link. If a solution exists for inverse kinematics problem, specified output is said to be within the workspace of the manipulator. Inverse kinematics of a serial manipulator is not very trivial. It involves solution of high order polynomials and transcendental equations and results in multiple solutions. It becomes easier, however, if the last three joint axes are intersecting and a generalized scheme for that case was first developed by Pieper (see pp 112 of Craig [1]).

The inverse kinematics of parallel manipulators can be considered to have the same complexity as that of serial manipulator, because the problem can be solved independently within each individual kinematic branch and hence the methodology of inverse kinematics of serial manipulators can be applied directly. However, in the presence of multi-dof joints, the inverse kinematics of parallel manipulators can be even simpler.

1.3 Objective of this Thesis

A three-DOF planar parallel manipulator is shown in Fig. 1.2. It consists of seven movable links connected with revolute joints which allow the positioning and the orientation of the platform in a plane. The potential applications of this manipulator are welding, deburring,

milling, pick and place operations over a planar surfaces and in assembly as a horizontal workstation. Designing, developing and understanding the behavior of the 3-DOF planar parallel manipulator is the aim of the research reported in this thesis.

1.4 Literature Review

The term "parallel manipulator" was first introduced by Marvin Minsky [2] of the MIT in his early AI memo "Manipulator design vignettes". According to his memo, the parallel concept is best illustrated by the way an animals body is supported by its legs, where several constraints simultaneously determine the relationships of one body to another.

Probably the most famous parallel manipulator is the Stewart platform. It was originally proposed by Stewart in 1965 [3] as a flight simulator, and versions of it are still commonly used for that purpose. Since then, the Stewart platform has also been used for other applications such as milling machines, pointing devices, and an underground excavation device. Generally, the Stewart platform has six limbs, where each limb is connected to both the base and the moving platform by spherical joints located at each end of the limb. Actuation of the platform is typically achieved by changing the lengths of the limbs.

The planar 3-DOF manipulator was introduced by Hunt in 1983 [4], which could be considered as a planar example of the well-known Stewart platform [3]. The planar 3-DOF parallel manipulator is an 8-bar linkage with two ternary links (frame and end-effector) connected through three in-parallel legs, each leg consisting of two links. Though a number of mechanisms are possible by different combinations of revolute and prismatic joints at the legs, two of them having 3-RRR and 3-RPR structures have attracted wide research interest, the later showing greatest similarity with the Stewart Platform.

Pennock and Kassner [5] studied the solutions to the total and primary workspace problem of the 3-DOF parallel manipulator. They derived a set of equations that determine the workspace as a function of the platform orientation. The reachable positions of the end-effector for a specified platform orientations are analyzed. They discussed the total primary workspace and the influence of special manipulator geometry on the workspace.

Ma and Angeles [6] studied direct kinematics and dynamics of planar 3-DOF parallel manipulator. In their method one of the links of the manipulator is removed virtually so that only one of the three kinematic loops remains. Which reduces the non-linear constraint equations from three to one and a technique of 4-bar linkage performance evaluation applied to find the position of end effector. In the dynamics formulation, the natural orthogonal complement is applied, which leads to the algorithm oriented equations of motions involving

independent generalized coordinates.

Gosselin and Merlet [7] made an alternative formulation for the direct position kinematics problem, developed robust schemes for the solution and established sharp upper bounds (less than 6) for specified geometries of the manipulator.

Gosselin and Angeles [8] described four different criteria for the optimum design of planar 3-DOF parallel Manipulator. These criteria are (a) symmetry (b) the existence of the non-vanishing workspace for every orientation of the gripper (c) the maximization of the global workspace and (d) isotropy of the Jacobian of the manipulator.

Kumar [9] described the reachable workspace, dextrous workspace of a parallel manipulator. He proposed an algorithm for finding the dextrous workspace of parallel manipulator and he discussed about the controllably dextrous workspace of a Parallel manipulator.

The dynamics of the parallel manipulator with revolute joints has been studied by Ma and Angles [6] by the method of orthogonal complement, while Revathi et.al. [10] described the Lagrange-Euler formulation for the dynamics of 3-DOF planar parallel manipulator with prismatic actuations.

1.5 Organization of the Thesis

The organization of the thesis is as follows.

The next chapter introduces some aspects like inverse kinematics, workspace and singularity analysis of 3-DOF planar parallel manipulator.

The third chapter deals with the kinematic and structural design and development of 3-DOF parallel manipulator. It also discusses the material selection and motor selection.

The fourth chapter deals with the control of motors, software and hardware implementation required for 3-DOF planar parallel manipulator.

The fifth chapter discusses results of the prototype manipulator developed in the present work.

The concluding remarks and suggestions for further work have been given in sixth chapter.

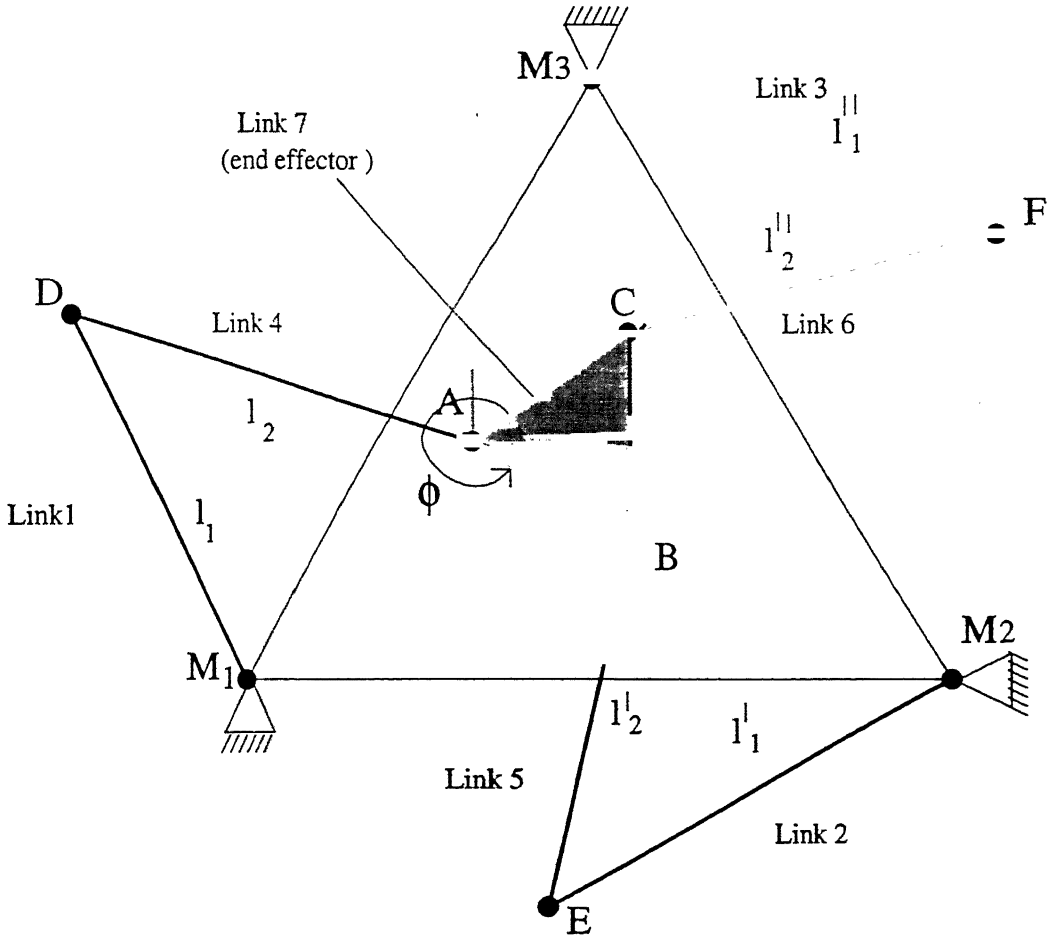

Figure 1.2: 3-DOF Parallel Manipulator

Chapter 2

Workspace and Singularity Analysis of 3-DOF Planar Parallel Manipulator

2.1 Symmetry Considerations

Unlike the case of an ordinary mechanism, which, most of the time, is designed for a specific task, the precise tasks to be performed by a manipulator are unknown a priori. Hence, there should not be any preferred general orientation for which the manipulator would have better properties. If it were designed for a particular task, it may have bad properties in some other configurations. This suggests that the manipulator should be symmetric, which shows equal performance in all the configurations.

The manipulator shown in Fig. 1.2 is composed of seven movable links, all the joints are of the revolute type and the motors M_1, M_2, M_3 are fixed. The motion of all links takes place in one plane. The manipulator consists of a kinematic chain with three closed loops namely M_1DABEM_2, M_2EBCFM_3, M_3FCADM_1 and the gripper is rigidly attached to triangle ABC. By symmetry, then the motors will be located on the vertices of an equilateral triangle and the link lengths will be same for each leg, i.e.

$$l_i = l_i' = l_i'', \quad i = 1, 2, 3$$

From a geometric viewpoint, this manipulator consists of three serial manipulators all of which have common base and end-effector. The three motors are placed at the vertices of the equilateral triangle of unit side.

2.2 Inverse Kinematics

The inverse kinematics problem is to compute the joint angles of the actuated links, given the position and orientation of the end-effector. The Cartesian coordinates of the gripper are given by the position of its centroid C (x, y) and the angle Φ defining its orientation. The inverse kinematic problem consists of determining θ_1, θ_2, θ_3 (joint variables) for given values of x, y, Φ. The solution to this problem contains eight different branches, i.e. two branches per leg since the solutions for the input angles θ_1, θ_2, θ_3 are completely uncoupled. For instance, the solution for the first leg is shown in Fig.2.1 . This solution is given, for leg i, by

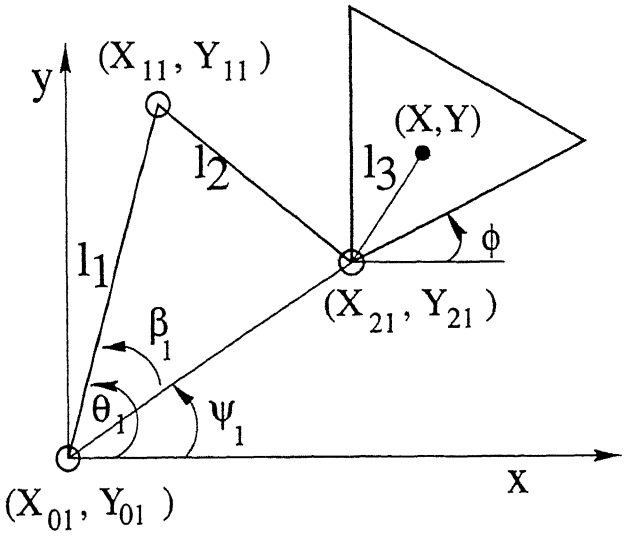

Figure 2.1: Analysis of the First leg

$$x_{2i} = x - l_3 cos\Phi_i - x_{0i}$$

$$y_{2i} = y - l_3 sin\Phi_i - y_{0i}$$

where angles $\{\Phi_i\}_1^3$ are given by

$$\Phi_1 = \Phi + \pi/6$$

$$\Phi_2 = \Phi + 5\pi/6$$

$$\Phi_3 = \Phi - \pi/2$$

and

$$\{x_{0i}\}_1^3 = \{0,\ 1,\ 1/2\}$$

$$\{y_{0i}\}_1^3 = \left\{0,\ 0,\ \sqrt{3}/2\right\}$$

consequently,

$$\theta_i = \psi_i \pm \beta_i$$

$$\psi_i = tan^{-1}\frac{y_{2i}}{x_{2i}}$$

$$\beta_i = cos^{-1}\frac{l_1^2 + x_{2i}^2 + y_{2i}^2 - l_2^2}{2l_1\sqrt{x_{2i}^2 + y_{2i}^2}}$$

2.3 Workspace

The total (or reachable) workspace of a planar manipulator is the area that comprises all points which a specified point fixed in the end-effector can reach. The dextrous (primary) workspace is the set of points in the reachable workspace at which the end-effector can assume all attitudes with its reference point coincident with the specified point. The boundary of the workspace is attained whenever at least one of the chain reaches its maximum or minimum length.

The solution of the inverse kinematic problem developed above can be used to describe the workspace of the parallel manipulator. For a given orientation of the end-effector, the workspace of the parallel manipulator in Cartesian space can be described as the intersection of three regions, each being the difference of two concentric circles. In order to obtain the center of circle of i-th chain (x_{ci}, y_{ci}), the vector $[b_i]$ has to be subtracted from (x_{0i}, y_{0i}) as shown in Fig. 2.2. The smaller circle is obtained with radius $r = |l_1 - l_2|$ and the larger

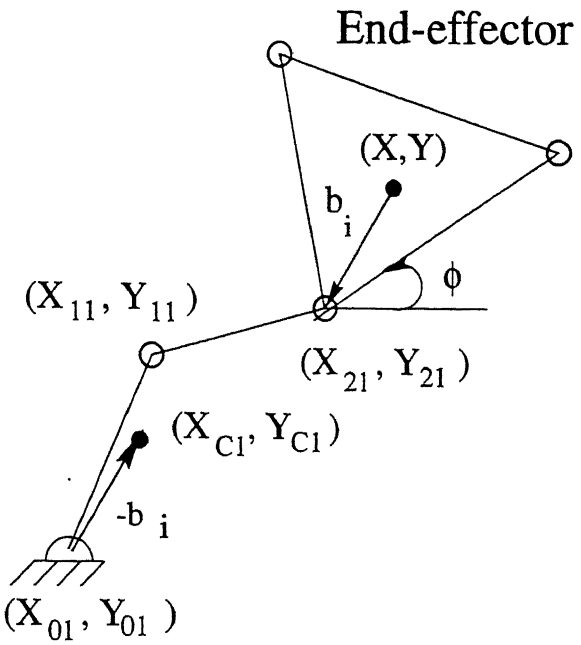

Figure 2.2: Location of Center of each of Circle to Compute Workspace

one with radius $R = l_1 + l_2$. The position of the centers of the circles will depend on the kinematic parameters of the manipulators and on the orientation specified for the platform.

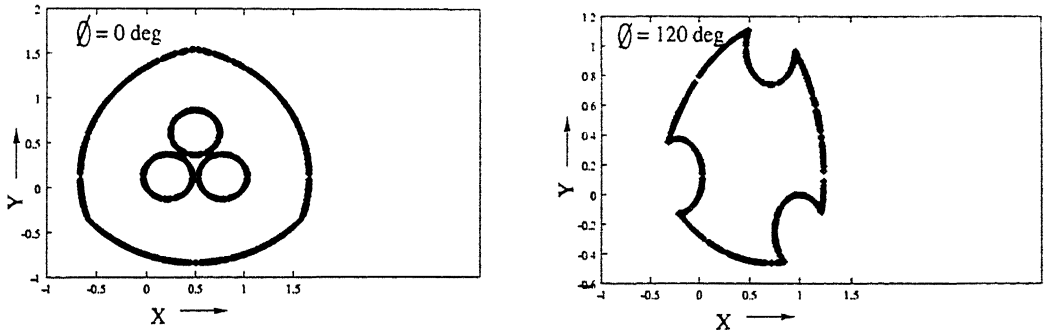

Figure 2.3: Workspace with Different Orientations

The workspace of the 3-DOF planar parallel manipulator depends on the platform orientation. Fig. 2.3 shows the workspace of a manipulator ($l_1 = 0.6$, $l_2 = 0.85$, $l_3 = 0.2$) with two different orientations. The algorithm used to evaluate the workspace incrementally moves the end-effector and then solve the inverse kinematics. If the inverse kinematic solutions exist that means the point is in workspace and all the points are stored in a file and the Fig. 2.3 was drawn.

2.4 Singularity

Singular configurations are those configurations in which the Jacobian matrices are degenerate, i.e those matrices relating input speeds with output speeds become rank deficient. In those configurations, the DOF of the system changes locally. The singularity analysis of parallel manipulators is more difficult compared to serial manipulators because of one or more closed kinematics loops and a number of passive joints.

2.4.1 Singularity Analysis using Jacobian Matrix

Gosselin and Angeles [11] developed a technique for evaluating the singularities of closed loop mechanisms. Let $\boldsymbol{\theta}$ and $\mathbf{X}$ be the vector of joint coordinates (input) and vector of Cartesian coordinates of the $n-$DOF parallel manipulator respectively.

$$\boldsymbol{\theta} = [\theta_1 \ \theta_2 \ldots . \theta_n]^T$$

$$\boldsymbol{X} = [X_1 \ X_2 \ldots X_n]^T$$

where θ_i is the variable associated with displacement of a prismatic joint or with the rotation of revolute joint. Similarly X_i is a component of position and orientation in Cartesian space. The input-output relationship between them can be described in general as

$$\mathbf{f}(\boldsymbol{\theta}, \boldsymbol{X}) = \mathbf{0} \tag{2.1}$$

where 0 is the n-dimensional zero vector. Differentiating the above with respect to time, one obtains

$$\boldsymbol{A}\dot{\boldsymbol{X}} + \boldsymbol{B}\dot{\boldsymbol{\theta}} = 0$$

where $\mathbf{A} = \partial \mathbf{f}/\partial \mathbf{X}$ and $\mathbf{B} = \partial \mathbf{f}/\partial \boldsymbol{\theta}$ are $n \times n$ matrices which are configuration-dependent. These matrices are called Jacobian matrices. Singularities of parallel manipulators are broadly classified into two types.

Singularity of type I

This type of singularity will occur when we have

$$det\,(\mathbf{B}) = 0$$

This type of singularity consists of the set of points where at least two branches of the inverse kinematics problem meet. This problem being understood here as the computation of the values of the driving joint variables from given values of Cartesian variables. Since nullity of **B** is not zero, we can find a set of non-zero actuator velocity vectors $\dot{\theta}$ for which Cartesian velocity vector $\dot{X}$ is zero. In other words, some velocities cannot be produced at the end effector, the manipulator thus loses one or more DOF.

Singularity of type II

This will occur when matrix **A** is rank deficient, i.e.

$$det\,(\mathbf{A}) = 0$$

This corresponds to the configurations in which the gripper is locally movable even when all the actuated joints are locked. This type of degeneracy can occur inside the Cartesian workspace of manipulator and will correspond to the set of configurations for which the direct kinematics of two different branches will meet. This type of singularity will occur only in parallel manipulators and not in serial manipulators because the direct kinematic problem of serial manipulator always leads to unique solution. Since the nullity of **A** is not zero, we can find a set of non zero Cartesian velocity vectors $\dot{X}$ for which the actuator velocity vector $\dot{\theta}$ is zero. Then the mechanism gains one or more DOF and becomes uncontrollable, or equivalently cannot resist forces or moments in one or more directions even if all the actuators are locked.

2.4.2 Singularity Analysis of 3-DOF Planar Parallel Manipulator

For the 8-bar 3-DOF planar parallel manipulator shown in Fig. 1.2,

$$\mathbf{X} = \begin{bmatrix} t \\ \Phi \end{bmatrix} = \begin{bmatrix} x \\ y \\ \Phi \end{bmatrix}, \quad \theta = \begin{bmatrix} \theta_1 \\ \theta_2 \\ \theta_3 \end{bmatrix}$$

and the kinematic input-output equations become

$$\|\mathbf{t} + \Re\,\mathbf{p}_i - \mathbf{b}_i - l_1\,\mathbf{C}_i\| = l_2 \quad for\, i = 1,2,3$$

where $\Re = \begin{bmatrix} cos\Phi & -sin\Phi \\ sin\Phi & cos\Phi \end{bmatrix}$ $\qquad$ $\mathbf{C}_i = \begin{bmatrix} cos\theta_i & sin\theta_i \end{bmatrix}^T$

Here, x, y, Φ denote the position and orientation of the platform relative to the base, while $(b_{ix}\ ,\ b_{iy})$ and $(p_{ix}\ ,\ p_{iy}\ )$ denote the i–th base point and platform point in the respective frames of references.

The above equation is in the form

$$\boldsymbol{F}\,(\,\boldsymbol{\theta}\,,\,\boldsymbol{X}\,) = \mathbf{0}$$

By differentiating with respect to time we can obtain Jacobian matrices **A** and **B**,

Singularity of type I occurs when matrix B becomes rank-deficient. This type of configuration is reached whenever the links of lengths l_1 and l_2 of one of the legs are aligned.

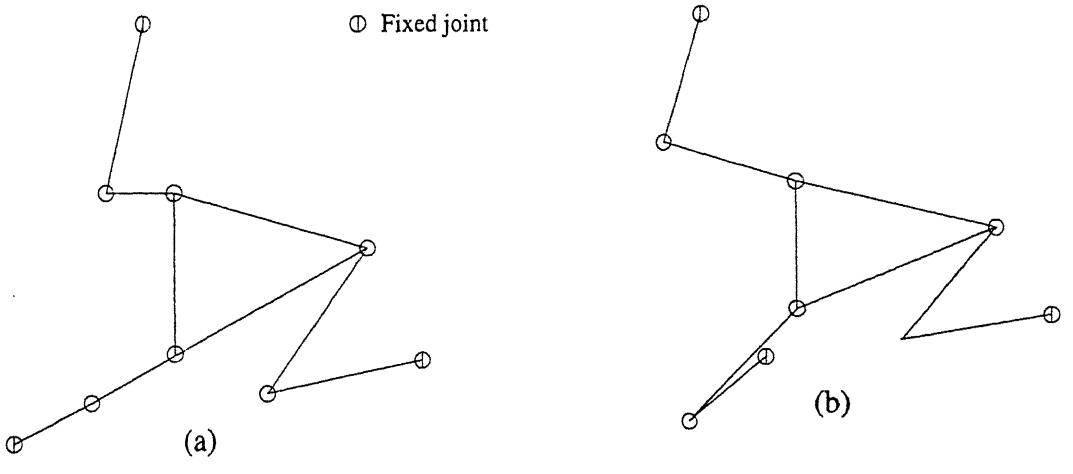

(a) one leg fully extended. (b) one leg fully folded.

Figure 2.4: Examples of type I of Singularity for the 3-RRR Manipulator

That corresponds to the fully extended or fully folded leg which does not produce any motion along the axis of corresponding leg shown in Fig. 2.4. This is, in fact, the boundary of the Cartesian workspace (where inverse kinematic solutions of the leg meet) .

Singularity of type II occurs when matrix **A** becomes rank-deficient. This type of singularity is found only in parallel manipulators, which is often inside the workspace of the manipulator.

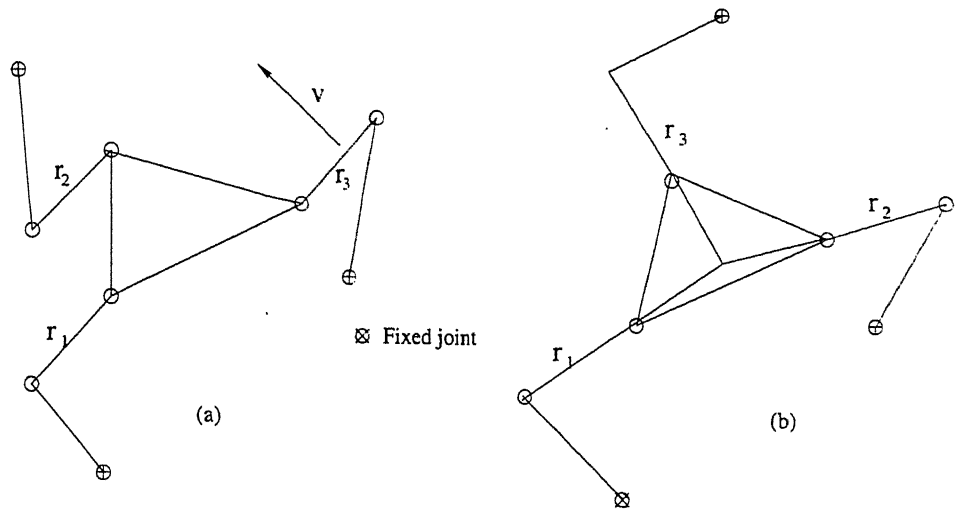

(a) Three vectors r_i are parallel (b) Three vectors r_i intersect at a point

Figure 2.5: Examples of type II of Singularity for the 3-RRR Manipulator

This type of singularity occurs in two different cases. The first occurs when the lines along each of three links of length l_2 are parallel. The platform can move along the direction V (Perpendicular to r_i, refer Fig. 2.5) even if the actuators are locked. Likewise a force applied to platform in that direction cannot be balanced by the actuators. The second case is for the configurations for which the vectors in the direction of links of lengths l_2, intersects at a common point. The platform can rotate about that point even if all the actuators are locked. Likewise a moment applied to platform cannot be balanced by the actuators. These are shown in Fig. 2.5.

2.4.3 Measure of Manipulability

Since singular points are found not only on the boundary of the workspace, but also inside it, they limit the end effector trajectories that a manipulator should follow in solving inverse kinematics. However, the most serious problem of singularity is not only at singular points, which have zero volume in the workspace, but rather in the neighborhood of the singular points. In parallel manipulator singularity of the first type are known to happen usually at the boundary of the workspace. The main difficulty is due to singularities of second type which is found inside the workspace where motion of the end-effector is possible even if the actuators

are locked. This causes a large error in end-effector motion. At singular configurations, the determinant of Jacobian matrix is zero. So it is natural to use the determinant of Jacobian in a measure of manipulator dexterity. Yoshikawa [12] introduced the measure of manipulability to evaluate quantitatively the kinematic ability of robot manipulators (see also Nakamura [13]). The measure of manipulability w is defined as

$$w = \sqrt{det\{\mathbf{J}(\boldsymbol{\theta})\,\mathbf{J}^T(\boldsymbol{\theta})\}}$$

The measure of manipulability becomes zero at singular points and takes positive values elsewhere. Since the measure of manipulability changes continuously (Jacobian depends on configuration) as the robot moves, it can be considered as a kind of distance from singular points. From above, a good manipulator design has large areas of its workspace characterized by high values of w. In parallel manipulators, two Jacobian matrices are involved. For parallel manipulator the measure of manipulability can be taken as

$$w = \sqrt{det\{\mathbf{A}\,\mathbf{A}^T\} + k * det\{\mathbf{B}\,\mathbf{B}^T\}}$$

where k is a factor that determines the contribution of the term $det\left\{\mathbf{B}\,\mathbf{B}^T\right\}$ to maximize in the above equation.

2.4.4 Home Configuration

The volume of mobility being symmetric about the centroid of the triangle defined by the location of the motors, this point of the x-y plane is the one where the manipulator attains the maximum mobility in terms of the different values of the angle Φ that it can reach. Therefore this position is the one at which we would like the Jacobian to be well conditioned. We call this position as home configuration. This is often defined as that in which the centroid of the gripper is located at the centroid of the base triangle.

From above a good manipulator design has a large value of w in the home configuration.

Chapter 3

Design Details

3.1 Design of Link Lengths

The Jacobian matrices of the parallel robot depend on its orientation. For a fixed orientation the Jacobian matrices depend on the link lengths of the manipulator. For a good design the link lengths of the manipulator should be such that its measure of manipulability is maximum.

The lengths of all the links are calculated such that the measure of manipulability w is maximum in home configuration, which is far from singular configurations. By taking the distance between two fixed joints of base triangle as unit distance, the link lengths are determined using optimization technique to maximize w.

3.1.1 Optimization Procedure

The optimal design of a parallel manipulator involves the design of links using any optimization technique. There are two types of optimization techniques, one is unconstrained optimization and the other is constrained optimization. The general non-linear constrained optimization problem can be stated as follows :

Minimize $F(X)$ (Objective function)

Subject to

$g_j(x) \geq 0, \quad j = 1 \ldots .m$ (Inequality constraints)

$h_k(x) = 0, \quad k = 1 \ldots .n$ (Equality constraints)

$x_i^{(L)} \leq x_i \leq x_i^{(U)}, \quad i = 1 \ldots .N$ (Decision variables)

This is the most general form of single objective constrained optimization problem. There are N decision or design variables, in which the lower and upper bounds are specified.

There are m inequality constraints and n equality constraints in the above problem. For a maximization problem, the above objective function $F(X)$ can be transformed into $-F(X)$ by multiplying the objective function by -1. This constrained optimization problem can be transformed into an unconstrained problem by using transformation methods.

As the present work involves the constrained maximization problem, the penalty function method [14] is used to transform the constrained optimization problem into unconstrained optimization by adding the penalty terms for each constraint violation. There are different penalty terms, among which the bracket operator penalty term is chosen to favor the selection of feasible points.

The penalty method works in a series of sequences, each time modifying a set of penalty parameters and starting sequence with the solution obtained in the previous sequence. At any sequence the following penalty function is minimized.

$$P(x, R) = F(x) + \Omega(R, g(x), h(x))$$

where $F(x)$ - objective function

Ω - Penalty term

R - Set of penalty parameters

$g(x)$ - inequality constraints

$h(x)$ - equality constraints

Bracket operator penalty

$$\Omega = R \langle g(x) \rangle^2$$

This penalty term is used for handling inequality constraints. Since the bracket operator assigns a positive value to the infeasible points, this is an exterior penalty term. The first sequence begins with a small value of the penalty parameter R and is increased in subsequent sequences.

Therefore the penalty function can be written as

$$P(x) = F(x) + \sum_j R \langle g_j(x) \rangle^2 + \sum_k [h(x)]^2$$

where $P(x)$ is unconstrained objective function known as penalty function.

The present problem is formulated for maximization of objective function and set of given inequality constraints using stated penalty function method as follows.

Maximize w

or

Minimize $-w$

Subject to

$$3\left(l_1+l_2\right)^2-\left(\sqrt{3}l_3+1\right)^2\geq 0$$

$$3\left(l_1-l_2\right)^2-\left(\sqrt{3}l_3+1\right)^2\leq 0$$

where w is objective function, which is the measure of manipulability to be maximized. The less-than -or-equal type constraints can be transformed into the other type by multiplying the constraint function by -1. The limitations of this work is that in w there are two terms i.e. $\mathbf{A}$ and $\mathbf{B}$, and our intention is that the determinants of each is far from zero. While optimizing the objective function, we may get a result such that determinant of one of the matrices is too far from zero and at the same time the other is near making the combination far from zero. Such a situation is not desirable. So by trial and error with the value of k in w, we obtain dimensions of links such that each of the matrices should be far from zero as well as the combination. For our case, the best design was achieved for a value of $k = 1.0$.

The results of the optimization are, three relative link lengths of 0.6, 0.85, 0.2. A suitable scaling factor is chosen, say 15 which results the link lengths of 9.0 cm, 12.75 cm, 3.0 cm. These sizes are adopted for the prototype.

Another possible approach to the above problem is by changing the objective function to

$$\sqrt{\frac{1}{det\left\{\mathbf{A}\,\mathbf{A}^T\right\}}+\frac{k}{det\left\{\mathbf{B}\,\mathbf{B}^T\right\}}}$$

and applying minimization techniques we can find the link lengths. In this, the value of k, we can take depending on the weightage of the terms and there is no need to check with every k to get the optimum results. But the difficulty is that while doing optimization if any singular configurations occur, a floating point overflow may occur because of division with zero.

Another way could be to change the objective function to

$$\sqrt{det\left\{\mathbf{A}\,\mathbf{A}^T\right\}*det\left\{\mathbf{B}\,\mathbf{B}^T\right\}}$$

and to maximize it.

The constraints used here are for existing of non-vanishing workspace for every orientation of end-effector [8]. The link lengths are calculated to satisfy the above constrained limits.

After finding link lengths the dimensions of links for a payload of W are calculated.

The payload of a robot is the maximum load which it can handle in any configuration of its linkage. Of course higher payloads can be handled in some configurations than they can be in other ones.

3.2 Structural Design and Analysis

Structural design consists of planning the physical construction of the load-carrying parts of the robot. Specifically, this task includes specifying the shape, cross section, and materials used for each link of the arm and also the actuators and transmissions.

Typically the designer begins at the end-effector of the manipulator designing the end link and its actuator-transmission to meet the applicable load, accuracy, speed, and other requirements. This link with its mass and reaction forces added to the applied load is used to design the next link, one step closer to the base. Subsequent links towards the base are designed until the design is complete.

This structural design which has proceeded one link at a time must now be subjected to an overall analysis to see whether it will perform as desired. Many performance features, such as the accuracy and overall stiffness, depend on all the joints and links and cannot be evaluated separately. Performance may also depend on the sensors and control system which are not yet specified. Representative values for unspecified quantities should be used.

There are two approaches to the overall structural design: Accuracy and Frequency. The accuracy approach is concerned with the structural stiffness and how it affects accuracy. The frequency approach is concerned with stiffness and inertia and how they affect the dynamics of the manipulator. Both approaches may be necessary to ensure that requirements have been met, although a single approach by itself is often sufficient since both approaches tend toward similar designs. Since the accuracy approach is simpler, it may be the only analysis used on simple manipulators.

3.2.1 Accuracy Analysis

The accuracy approach to the robot design assures that the endpoint of the manipulator is within the specified accuracy whether or not the robot has a payload. In general payload and accuracy are specified. The analysis amounts to a determination of the spring constant of the endpoint of the manipulator in various configurations. The manipulator must deflect less than the specified accuracy under the specified payload, i.e., a minimum spring constant is required.

3.3 Material Selection

The material for the links is selected on the basis of stiffness-to-weight ratio [15], high strength and low weight. To increase the stiffness-to-weight ratio, the increase in the elastic modulus E is very desirable, if it is not accompanied by an unacceptable increase in specific density ρ. Parameters of some high modulus and/or low specific density materials are discussed in [15]. Best properties are demonstrated by ceramics (boron carbide and aluminum) and beryllium. While ceramics are brittle and difficult to machine, beryllium is very costly. Fiber reinforced materials also have good stiffness-to-weight ratio but their applications are limited because of creep under constant constant load (for some compositions), aging, high thermal expansion coefficient, difficulty of joining with metal parts and high costs. Popular light structure materials as magnesium, aluminum and titanium have the same E/ρ ratios as that of steel [16]. Thus these materials are used where low weight with high strength is more important than E/ρ ratios. Thus considering all these factors aluminum is selected as material for the links.

After selecting the material for different links the dimensions of the links are calculated as follows. The dimensions are calculated for a particular payload W and accuracy δ. This payload is shared by all the three chains. If the load application point (center of end-effector) and the center of the base triangle coincides, the payload is shared equally by all the links. The load acting on each chain depends on configuration of the robot. This load acting (sharing) is proportional to the distance between the load application point (center of end-effector) and the base (fixed) joint of the respective chain. The design procedure for all three chains are the same because of the symmetry of all chains. Now the design problem is reduced to single chain. The load acting on a chain is maximum if the distance between the fixed joint and load application point of that chain is greater than that of other two chains. The design will be safe when it is designed for maximum loading conditions. The maximum load acting on a particular chain can be calculated as follows.

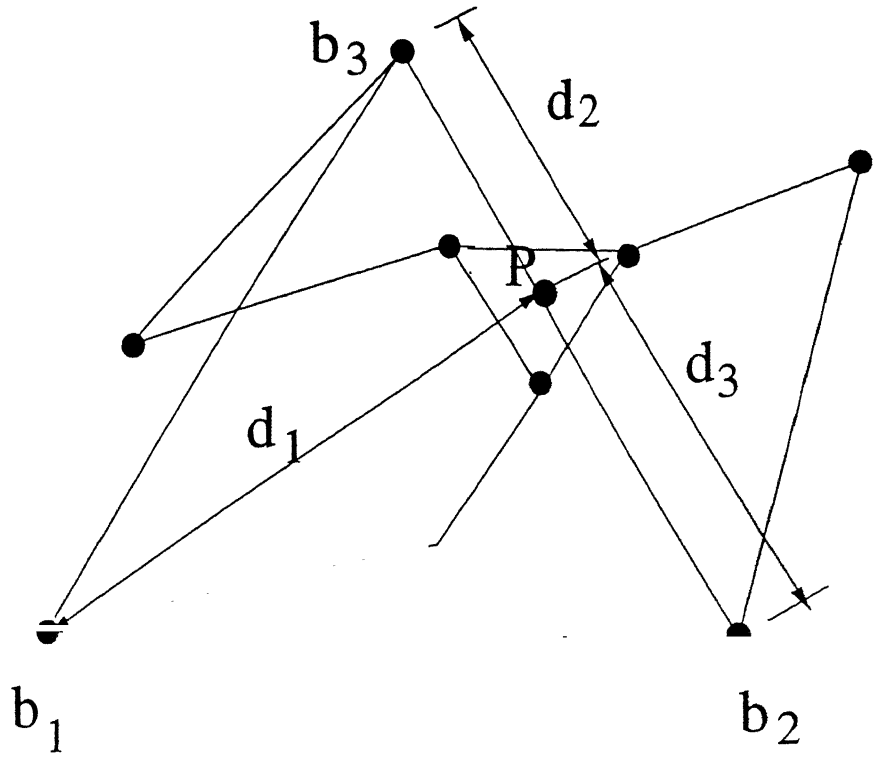

Figure 3.1: Load Sharing of each Chain

In Fig. 3.1, b_i is the base (fixed) joint of $i-$th chain. P is the position of the center of end-effector and d_i is the distance between the $i-$th base joint and center of end-effector (P).

The load acting on $i-$th link $= \frac{d_i}{\sum_{j=1}^{3} d_j} * W$
where W is the pay load of the robot.

From the geometry of Fig. 3.1, one can say that the maximum load that act on a chain is $W/2$. This is possible for the configurations for which the end-effector coincides with base joint of the any of the other links.

Design of end effector

End effector is fixed at point C, as it is only allowed to rotate in plane perpendicular to the load acting as shown in fig.

So, consider cantilever of beam CD of length l_3 and load w acting at point d.
Bending Moment at C (M) $= \mathrm{w} * l_3 + W_3 * l_3 * l_3/2$
where W_3 is the load per unit length of the end effector
For a rectangular cross-section, $Z = b_3 * h_3^2/6$

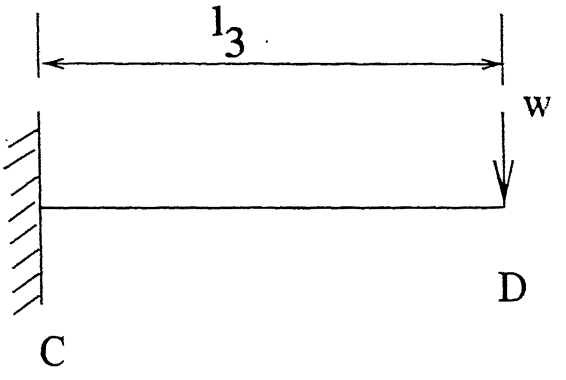

Figure 3.2: Loading on End-effector

Bending stress $f_b = M/Z$

The properties of the materials are known, so by choosing some thickness one can calculate the width of the link.

Design of the second link

Second link of the manipulator is connected between end effector and first link. The design procedure of this link is given below.

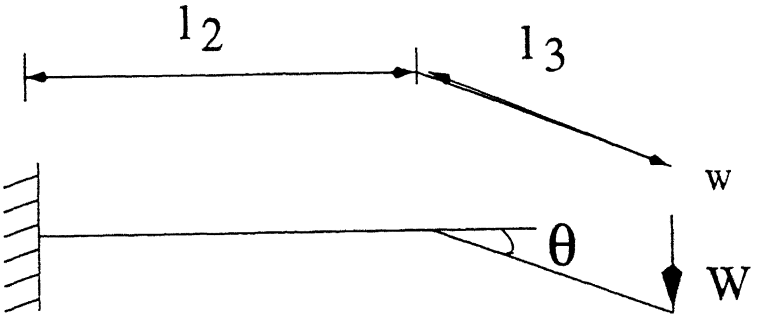

Figure 3.3: Loading on Second Link

The stresses acting on this link are torsional and bending stresses.

Bending moment is maximum when $\theta = 0$

$M_{max}\ at\ B = \mathrm{w} * (l_2 + l_3) + W_3 * l_3(l_2 + l_3/2)$

Bending stress $f_b = \frac{M_{max}}{Z}$

where Z = section modulus of the link 2

By knowing the material properties and maximum bending moment, one can find width of the link by choosing appropriate thickness.

Shear stresses will be developed due to twisting moment This torque is maximum when $\theta = 90°$.

$T_{max} = l_3 *$ w $+ W_3 * l_3 * l_3/2$

Shear stress $f_s = \frac{T_{max}}{J} * R$

where $R = \sqrt{\left(\frac{t}{2}\right)^2 + \left(\frac{b}{2}\right)^2}$

If the shear stress obtained is less than the f_{ys} then design is in safe condition.

Design of first link

To design the first link the same procedure stated above is followed. In design of first link the effect of the second and third links is also considered.

After calculating the dimensions of all the links, the overall deflection is calculated. If it is greater than the required accuracy then the same design procedure is followed until the accuracy obtained is less than the desired.

3.4 Basic Link Features

First Link

This link is fixed at one end of motor shaft and another end is connected with intermediate link. Two holes are drilled for joining these links with pins. At the end of Link 1 an internal thread and a slot is made as shown in Fig. 3.4. A long screw is passed through the internal thread. When the screw is tightened, link 1 tightly clamps the motor shaft. The purpose of this is to fix the link to motor shaft tightly without any relative motion. To avoid failure of the fixed end due to slot, it is required to keep more width when compared to another end.

The link dimensions are taken so as to minimize the deflection and stresses under loading.

Second link

One end of the second link is connected to first link and the other end is connected to the end-effector. This is the passive link in this manipulator. This link used in the present work is shown in the Fig. 3.5. Two holes are drilled in the link for joining it with other links.

End-effector

The end-effector in the present work is in the shape of equilateral triangle. The end-effector is connected to the second links of all chains and forms as closed loop. Three holes are

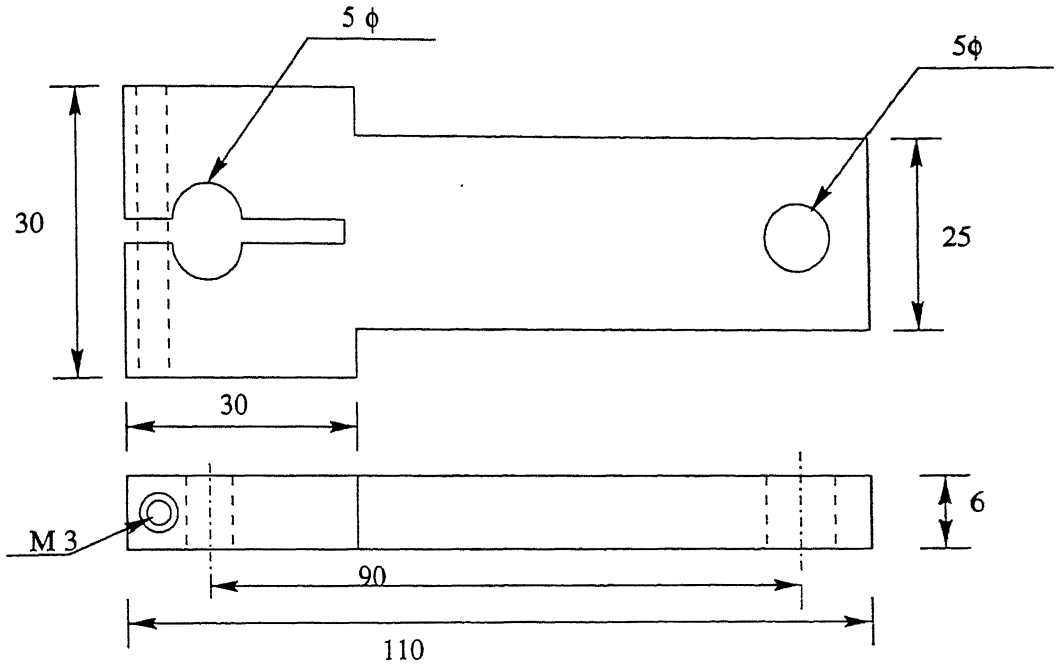

Figure 3.4: First Link

drilled for connecting links. Gripper is attached to the end-effector for doing tasks. The dimensions of end-effector used in this work is shown in Fig. 3.6.

All the links are joined with pin joints. A circlip is fitted to the pin to arrest vertical displacement. The method of joining is shown in Fig. 3.7.

The three motors are mounted on the stands such that the distance between any two of the motors is equal. The complete arrangement for one chain is shown in Fig. 3.8. Like this, all three chains are connected to the end-effector.

3.5 Motor Selection

After the mechanical structure of robotic manipulator is determined, a suitable actuator producing motion must be selected. The motors required to move the links of the manipulator must be having high torque-to-weight ratio. Also the motors should not be costly. For robotic applications two types of motors are generally used. That are Servo motors and Stepper motors. In the present work we used stepper motor because of the following advantages.

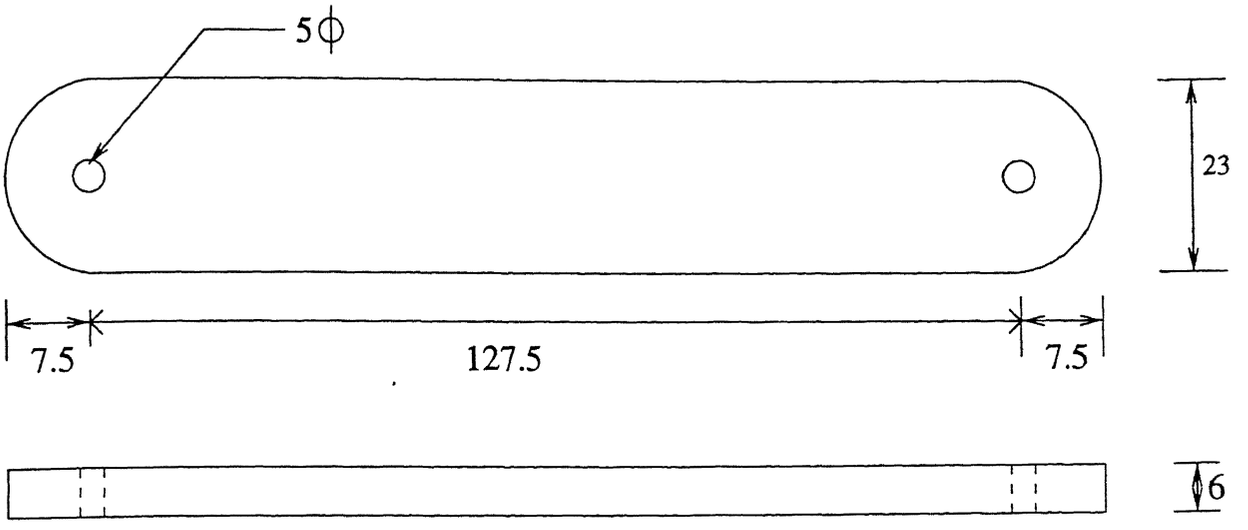

Figure 3.5: Second Link

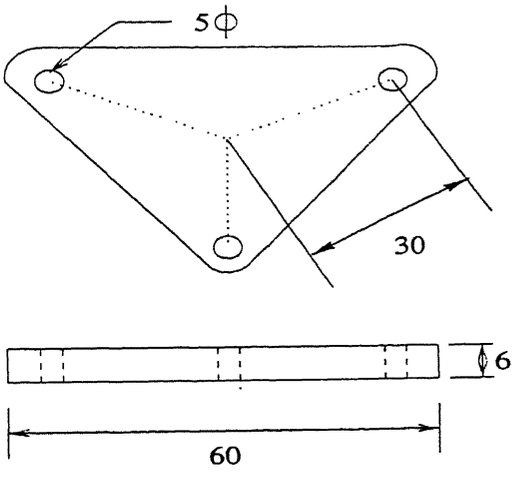

Figure 3.6: End-effector

3.5.1 Stepper Motors

Stepping motors are motors which convert electrical logic signals (pulses) to mechanical motion at a constant, defined angle. Each of these motions is called a step. The input of a stepper motor consists of a series of pulses, the rotor advances one step a pulse. The advantages of stepper motors compared to other motors are as follows.

1. Because of the fixed relationship between input signals and rotor motion, stepper motors do not require an encoder and servo controlled system in order to achieve the precise positioning required in robotic applications. Elimination of encoders and servo electronics results in a significant cost saving.

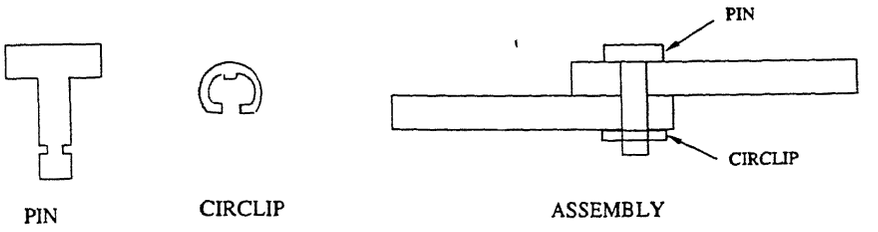

Figure 3.7: Joining links

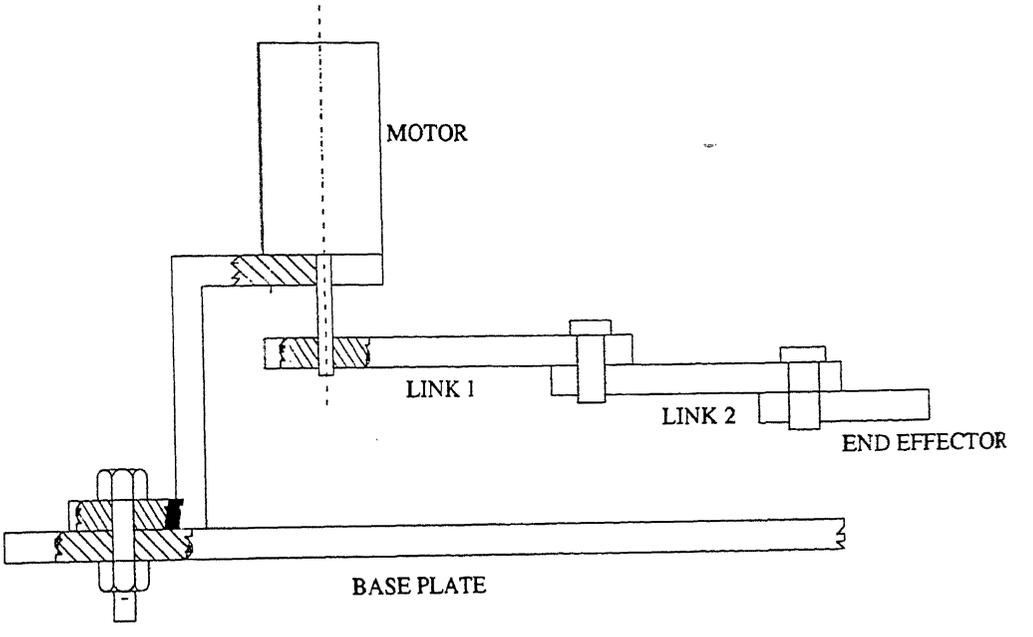

Figure 3.8: Overall Chain Assembly

2. Error in positioning a stepper motor is not accumulative as long as a fixed relationship between pulse and step is maintained.

3. They may be used at extremely low rates of revolution without mechanical transmissions, unlike other motors which require gears to reduce the rate of the rotor revolution.

4. They can produce high torques at low rates of revolution.

5. When there is no pulse input, the rotor will remain locked in the position in which the last step was taken, because at anytime two windings energized are always energized which lock the rotor electromagnetically.

6. Since there is no mechanical connection to the rotor, there is nearly no friction on the components (except the bearings on both sides). Therefore there is only a small amount of wear and motion is quiet.

The main drawback of the stepper motor is that for a given output torque or horsepower the weight of the stepper motor is greater than other types of motors used for the robots. That is why the stepper motors are not widely used in serial robots because the links of the robot has to bear this weight. However, in parallel manipulators the links need not carry the load of the actuator, it can be fixed to the base.

Stepping motors can be programmed in three parameters

(a) direction (b) speed (c) number of steps.

Chapter 4

Implementation

This chapter explains software and hardware implementation in the present work. Computers are used to program robots, and the programming is done off-line. That means the robot is not directly involved when programming takes place. By using off-line programming, the programmer has greater flexibility to carry out complex operations, and the time spent in programming is reduced. In addition the robot can remain in service while the programming takes place, thereby increasing its productivity.

4.1 Control System

A personal computer based control system has been developed for the prototype parallel manipulator. The block diagram of this system is shown in Fig. 4.1. The system contains three major components: a host computer, the motor driver boards, and the motors. Each board controls one motor, so a total of three boards are used. The function of the stepping motor controller is to supply the motor with logic signals, in order to implement stepping in desired direction. The controller receives a series of pulses. The number of pulses determines the extent of revolution of the motor, and their frequency determines the rate of revolution. The controller defines the strength of the pulses to enable them to turn the motor, and addresses the signals to the motor coils in accordance with the desired direction of rotation.

The stepping motor controller includes a series of electronic switches responsible for switching the voltage of the stator coils which constitute the stator phase. The driver circuit is built with power MOSFETS. Power MOSFETS are commercially available with wide range of operating currents, IRF 540, IRF 840 etc. Use of MOSFETS make the design of driver board very simple and adaptive for a wide range of motors with different torque ratings. As per the current requirements for a particular application, appropriate MOSFET can be used

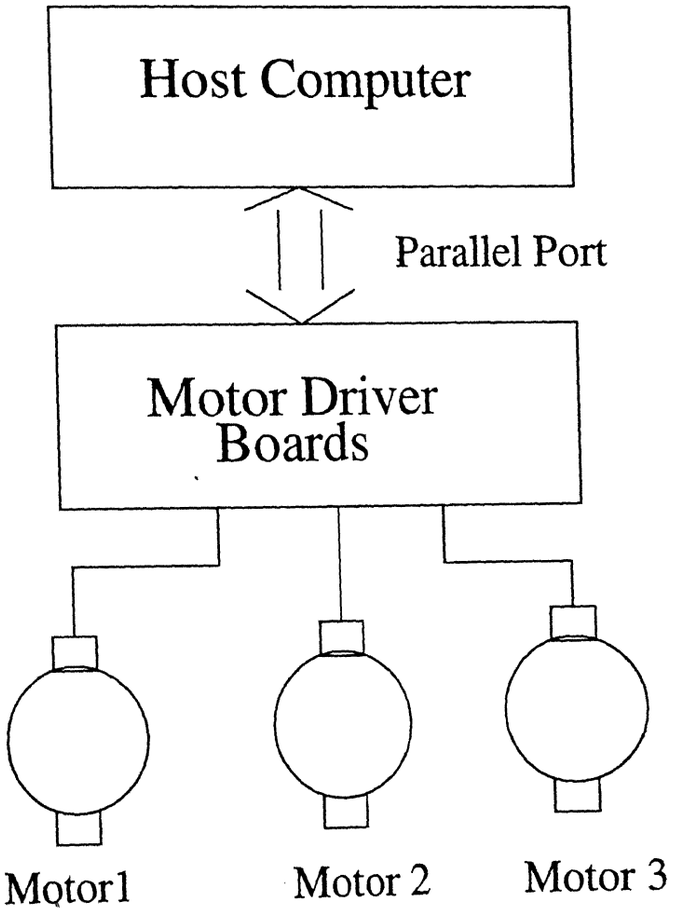

Figure 4.1: Control System Block Diagram

without any need to modify the printed circuit board (PCB) layout.

These circuits are discussed in detail in the following sections.

4.2 Bi-directional Logic Sequencer (BLS)

This is a circuit which utilizes digital integrated circuits (IC). It controls the excitation of windings sequentially, responding to the clock signal generated by the computer. This is capable of controlling the motor excitation in both directions, clockwise and anti-clockwise. The clock and the direction are the inputs of the circuit. Four outputs are generated which drives four phases of the motor. Fig. 4.2 shows the complete circuit diagram which uses IC 74LS73 (JK FF's) and IC 74LS51 (AOI) gates. IC 74LS73 is a negative edge triggered dual flip flop. It is configured to work in either load '0' or load '1' state by making $J = K'$ depending on the clock state. Oscillators output 'clock' is fed as the clock input to this IC

(both gates). It generates Q and Q' outputs which are used for two phases A, C (or ph1, ph3). These outputs are fed to IC 74LS51 (AOI) together with d (direction) and d' (inverted using IC 74LS04) pulses as shown in the circuit which are fed to the other similar gate hence producing the other two required outputs for B and D phases (or ph2, ph4). A, B, C, D outputs are generated in the sequence required for the rotation of motor. These signals are then buffered and used as input to the MOSFETS.

4.3 Driver Circuit

The driver circuit is rather simple. It uses four MOSFET's, each for one phase configured as a switch. A, B, C, D outputs generated in the BLS stage, each connected to a buffer gate (IC 74LS126) which enables with an active high signal. Buffered outputs called as BA, BB, BC and BD are each connected to the gate terminal of power MOSFET through a series resistance which biases the MOSFET. The phones (coils) of the stepping motors are connected between 12V power supply and the Drain terminal of MOSFET. Its source terminal is grounded. These MOSFET's are rated for 5A of peak current. Use of MOSFET's reduces the driver circuitry and makes it quite simple. Fig. 4.3 shows the circuit diagram for one phase. it is similar for other three phases also. A diode is put parallel with the winding in the polarity as shown in Fig. 4.3. This is particularly needed when fast switching is done. When MOSFET is turned OFF, a circulating current flows through the diode (otherwise producing the back emf) without damaging the MOSFET.

A PCB is designed using 'PCCARDS software'. A parallel port connector slot is provided to be able to drive the motor using personal computer. Two bits are needed to control one stepper motor (with the ground line). Speed of the motor is controlled with suitable delay between two clocks. Fig. 4.4 shows the PCB layout with the components. PCB's are fabricated, soldered and tested. Presently all three motors of the parallel robot are controlled by personal computer.

4.4 Interface with PC

Interfacing links permit the robot to communicate with its controller and other parts of workstation. Parts that do not cause the robot to do its task directly are called peripheral components. The microprocessor controlled robot can communicate with the equipment around it through connections called ports. For example, it is necessary for the robot to input information to the controller, and it must be able to receive information to the controller. Hence the

controller is connected to the robot through a port.

Parallel ports are the outputs of the microprocessor or computer that have flat cables connected to them with eight conductors. This parallel port is connected to the input of the controller circuit. The signals generated by the computer are fed to the controller circuit through the parallel port.

For generating signals, Turbo C provide access to the I/O ports on the 80x86 CPU via the predefined functions, inportb/inport and outportb/outport. For the present, work used outportb which outputs a byte to the hardware port. This is interface between program and stepper motor control circuit. The usage of outportb is as follows.

```
#include<stdio.h>
#include<dos.h>
#define Data 0x378
unsigned char Bits;
outportb(Data,Bits);          /* output data */
```

In the above program, 0x378 is the printer port address of port 1. Writing to this address causes data to be stored in the printers data buffer.

In 3-DOF parallel manipulator three stepper motors are used for activating the links. The controller circuit of each stepper motor needs two bits, direction and clk. To control all three motors 6 bits are required. The speed of the motors can be controlled by suitable delay between the two successive pulses. pulse rate is the number of steps per second. Step response time is the motor reaction time to an input pulse, causing it to move one step. This time determines the upper limit of the pulse rate. At pulse rates above this upper limit, the motor will not be able to react to each pulse, and deviation from the desired rate of revolution will occur. The delay between two pulses is such that the motor responds for each pulse.

In the present work, point to point control is used. Point to point control involves the positioning of the end-effector at given points, without dictating the exact course to be followed by the end-effector between these points. Applications for this method of control are those which require exact positioning of the end-effector at certain points at which the operations are to be carried out, provided the robot arm is at rest and not in motion during implementation of these operations. An example is spot welding. In point to point control first the initial and final positions of the manipulator are converted into joint space coordinates with inverse position kinematics. The computer sends signals to the motors until the motors move the joints to positions corresponding exactly to those values.

In parallel manipulators, the point to point control is not carried out in joint space because the direct kinematics of the parallel manipulator leads to more than one solution. This means that even if we move the motors required angles the end-effector is likely to go to a position other than the required one. Usually the end-effector goes to the nearest solution. For parallel manipulators the path is always planned in task-space and the path between the initial and final points is divided into a finite number of points. At each point inverse kinematics should be calculated. The motors are driven (controlled) such that the end-effector follows the intermediate points and finally it reaches the required position.

4.4.1 Software Description

As this model is meant for experimenting and evaluating the theoretical calculations, we have provided a friendly computer user interface for carrying out the task.

The interface mainly consists of taking the initial position of the end-effector in task space co-ordinate system from user. For finding the initial position of the end-effector, we provided a graph sheet setup beneath the end-effector (on base plate) with properly marked coordinate systems. This coordinate system is taken as global frame of reference and all the calculations are done with respect to this frame only. The next input is approx angles of the activating links. This is required because inverse position kinematics of the 3-DOF planar parallel manipulator will yield at most eight solutions. From these the solution nearest the user specified angles is selected. Next the user must enter the final orientation of the end-effector. The final position of the end-effector can be entered in the either of the following two ways.

1. In text mode the user can enter the coordinates directly.

2. In graphics mode the workspace of the manipulator with given orientation is displayed and the user can click the mouse at any point in the workspace.

A straight line path is planned between the initial and final points in Cartesian space. If the path does not exist within the workspace then the program asks for a valid via point, until a valid via point is entered. The path is divided into a finite number of points and at each point inverse kinematics is carried out. Accordingly the number of pulses required for the motors and the direction of rotation are calculated. At each point, depending on the state of the motor, a character string is calculated and this is called in outportb function to generate signals. The signals are generated and delivered to the controller circuits. The motors are moved as per the signals. Finally, the current joint angles are saved so that they can be used

in the next loop and the process is repeated. The loop is ended when all the intermediate points are finished. The final position reached can be verified on the graph sheet.

Flow chart for coordinated control of the manipulator is shown in Fig. 4.5. This flowchart is used to move the manipulator from one point to another point in the workspace.

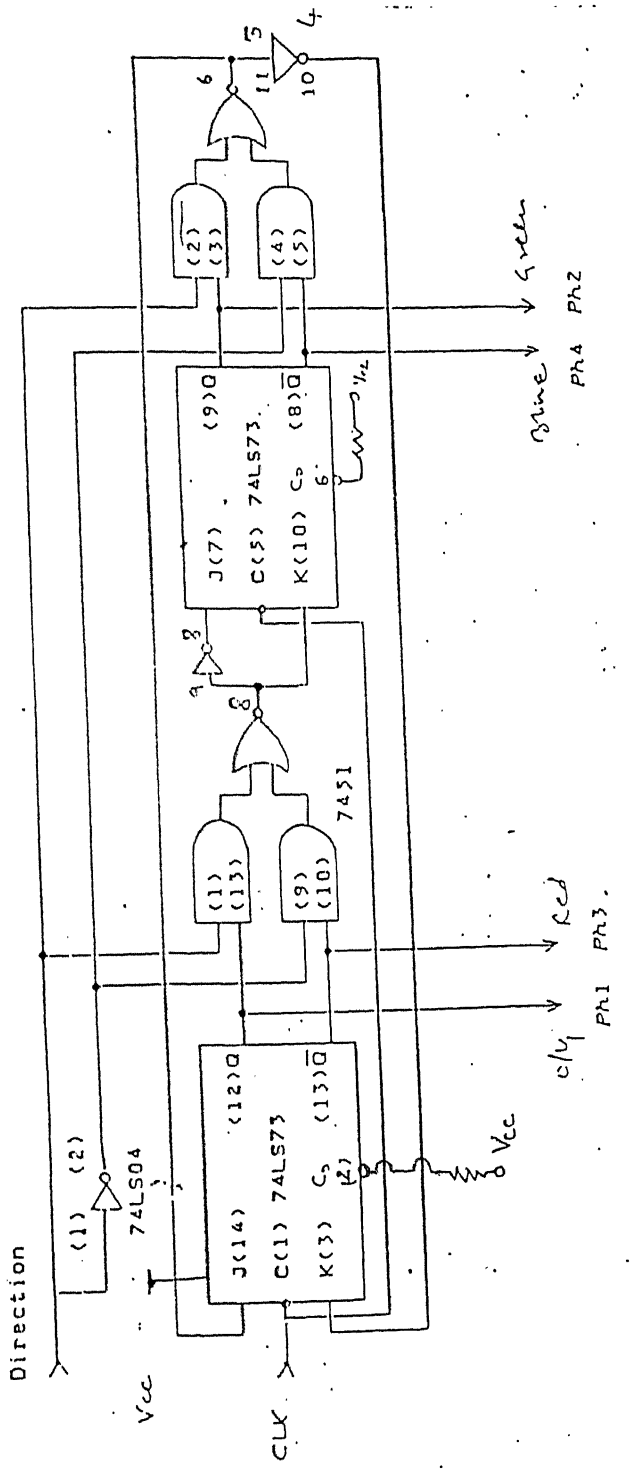

Figure 4.2: Bi-directional Logic Sequencer

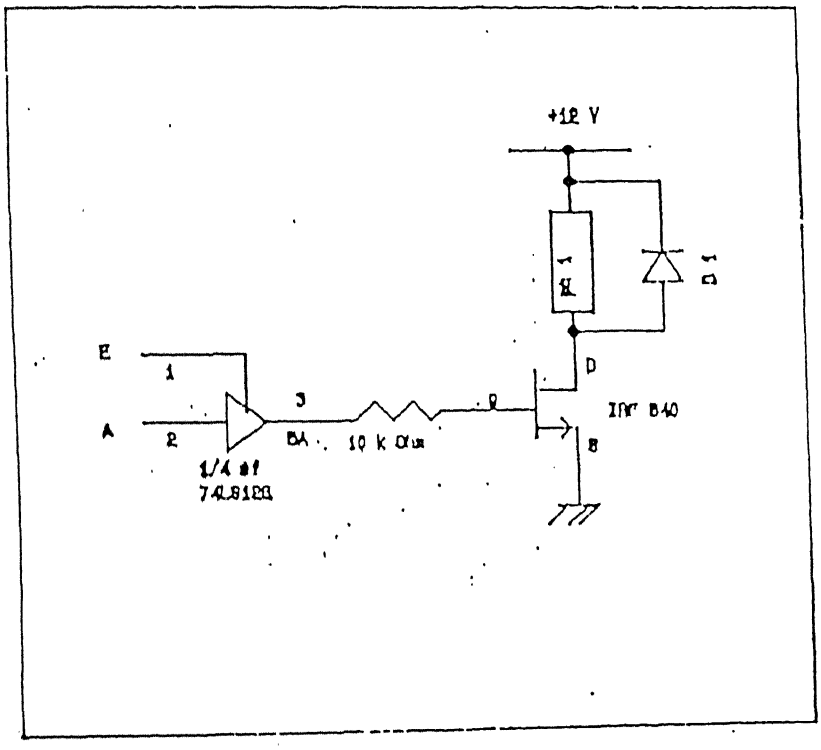

Figure 4.3: MOSFET Driver Circuit

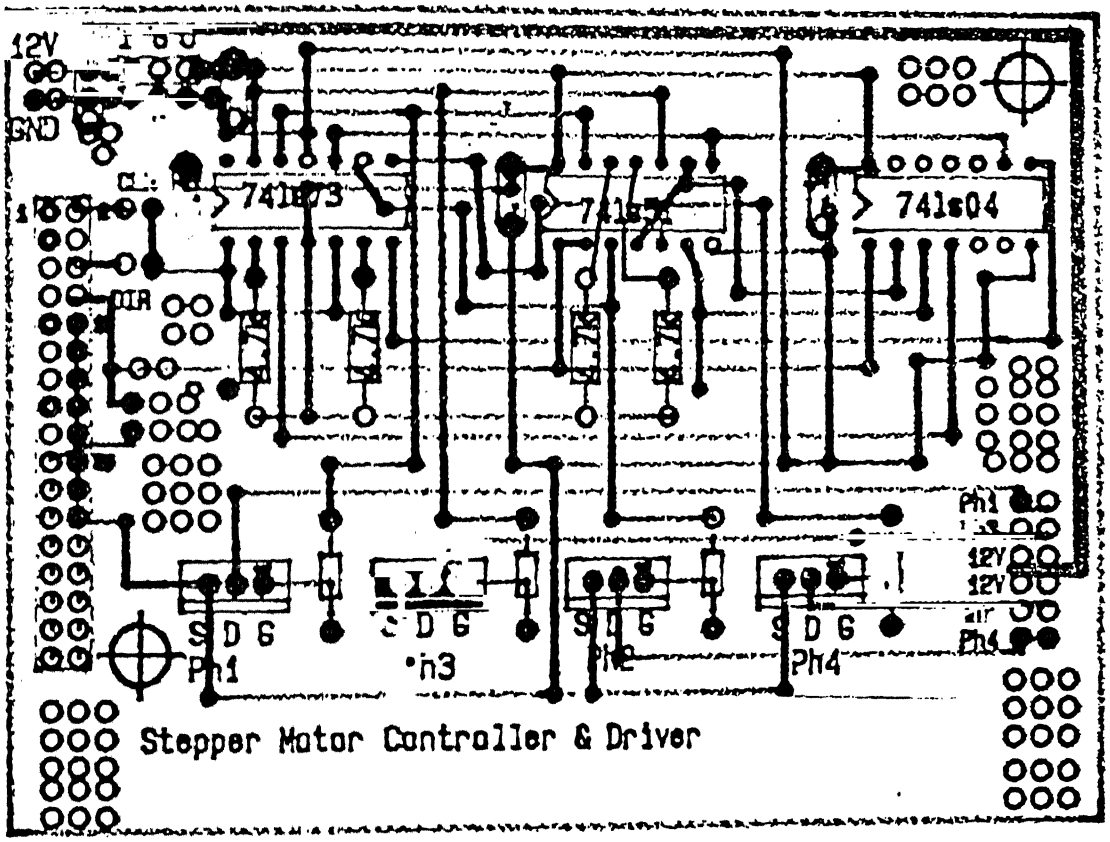

Figure 4.4: PCB Layout

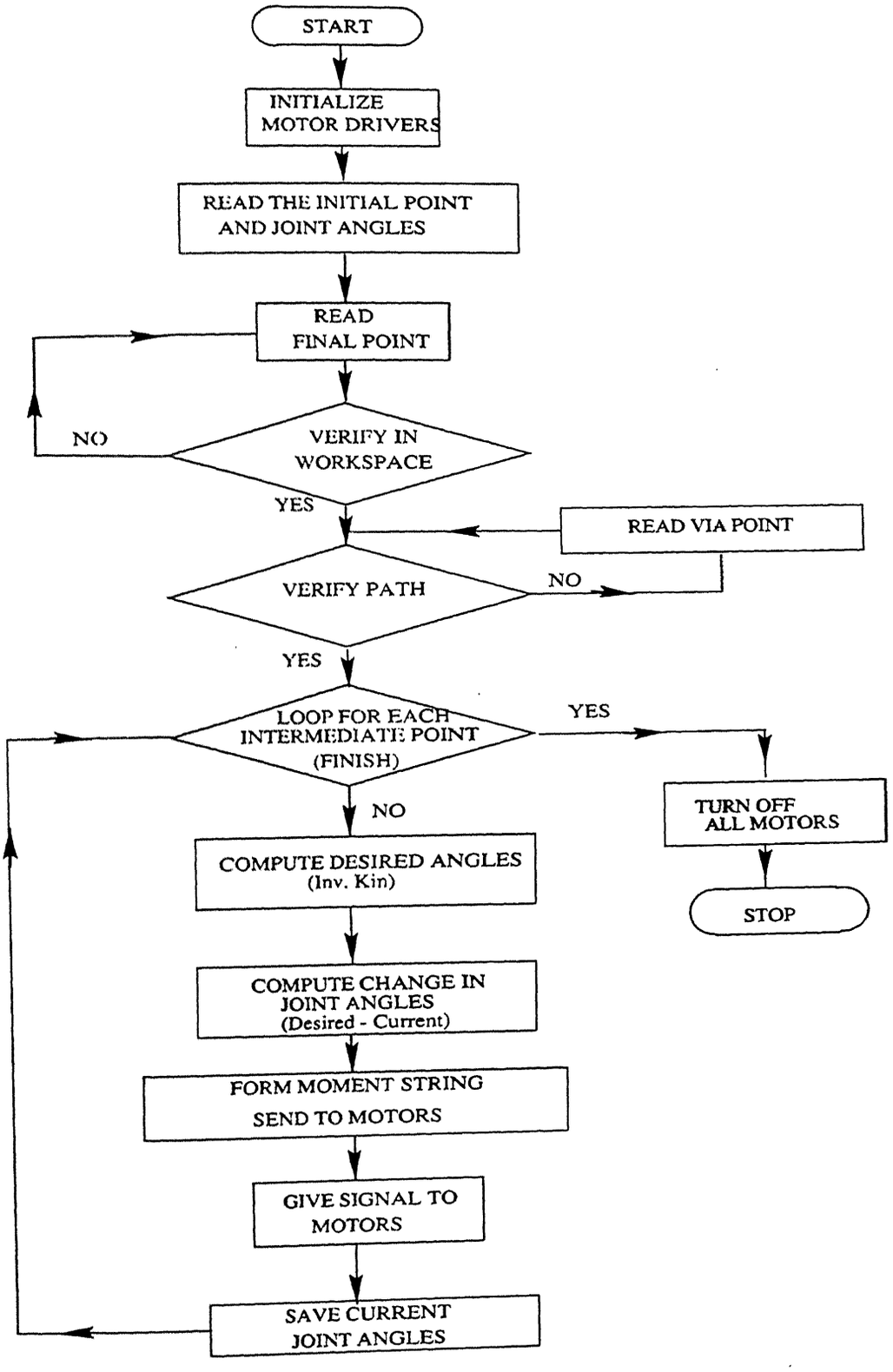

Figure 4.5: Control Flow-Chart

Chapter 5

Results and Discussions

5.1 Introduction

To investigate the basic characteristics of the 3-DOF planar parallel manipulator, a prototype manipulator was constructed. The general view of the 3-DOF planar parallel manipulator with revolute joints (that was constructed) is shown in Fig. 5.1, which is driven by stepper motors and controlled by a personal computer. In this work, position is controlled by counting and deducting pulses without the use of positional sensor and speed of the motors is controlled by careful application of pulse frequencies without use of a tachometric generator. The workspace of the prototype manipulator with different orientations of end-effector is shown in Fig. 5.2.

5.2 Accuracy

The accuracy of the robot depends on the resolution of the actuators. The actuators used in present work are stepper motors of 200 steps per revolution. That means the distance moved by the motor is in multiples of 1.8°.

The accuracy of the robot = $(1.8^* \pi/180) * L$

where L = effective length of chain.

At worst case L becomes sum of all the link lengths, when all three links of any chain are aligned, i. e. generally when the end-effector is at the outer boundary of the workspace.

Accuracy = $1.8 * \pi /180 * (9 + 12.75 + 3) = 0.77$ cm.

From above theoretically the accuracy of the robot is better than 7.7 mm.

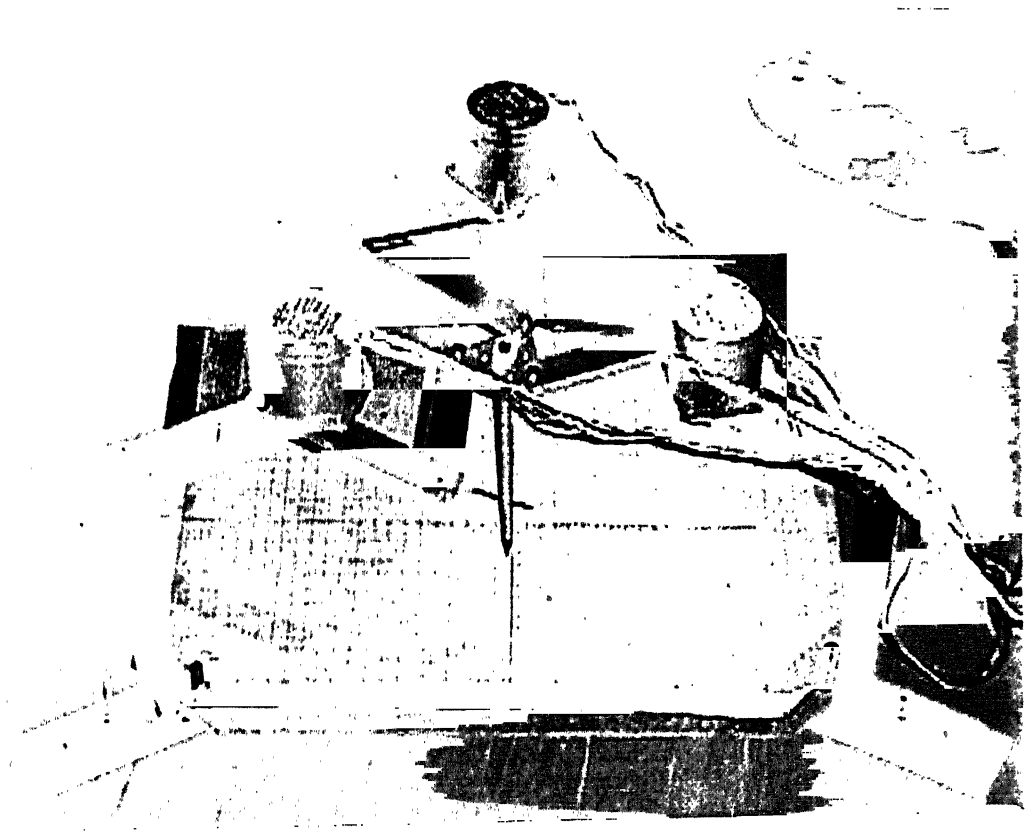

Figure 5.1: Prototype Parallel Manipulator

5.3 Performance Test

To determine the performance of our robot, we have conducted some experiments. In that we have given commands such that the robot moves from one point to another point and noted its performance regarding where it is going and what is the accuracy, repeatability of the robot.

5.3.1 Error in Positioning

Table 5.1: Performance Test

Initial Pos & Ori			Desired Pos & Ori			Reached Pos & Ori		
X (cm)	**Y** (cm)	Φ (deg)	**X** (cm)	**Y** (cm)	Φ (deg)	**X** (cm)	**Y** (cm)	Φ (deg)
0.2	-0.2	0	-4	-4	45	-3.8	-3.6	45
0.2	-0.2	0	-4	4	45	-3.7	4.1	40
0.2	-0.2	0	4	4	45	4	3	45
0.2	-0.2	0	4	-4	45	3.7	-4.5	40
-4	4	0	4	-4	0	3.5	-4.2	-10
4	-4	0	-4	4	0	-3.2	3.8	0
4	4	0	-4	-4	0	-3.5	-3.1	5
-4	-4	0	4	4	0	4	3.5	-5

Table. 5.1, shows the performance of the prototype manipulator. The error in positioning of the robot can be calculated as

Error in X direction E_x = X desired - X reached (in cm)

Error in Y direction E_y = Y desired - Y reached (in cm)

Error in Orientation E_Φ = Φ desired -Φ reached (in cm)

Combined error = $\sqrt{E_x^2 + E_y^2 + (E_\Phi * \pi/180 * L_3)^2}$ (in cm)

where L_3 is the length of the end-effector and in this work it is 3.0 cm.

The maximum error in positioning of this prototype manipulator is around **1.24 cm.**

This error is mainly due to the following reasons.

1. Inaccuracies (tolerances) in dimensions of mechanical links. It is very difficult to manufacture links with required dimensions exactly.

2. Motors move in terms of steps, so it is not possible to move the motor exactly as what we required and it is moved in terms of 1.8° .

3. Error in measurement of position and orientation of the platform.

4. Unavoidable slip between motor shaft and link.

5.3.2 Repeatability

The repeatability, one of the most important characteristics of any robot, is its ability to repeat its performance over and over again accurately.

The points shown in Table 5.1 are moved repeatedly a number of times and it was found that the manipulator is moving with 70% repeatability.

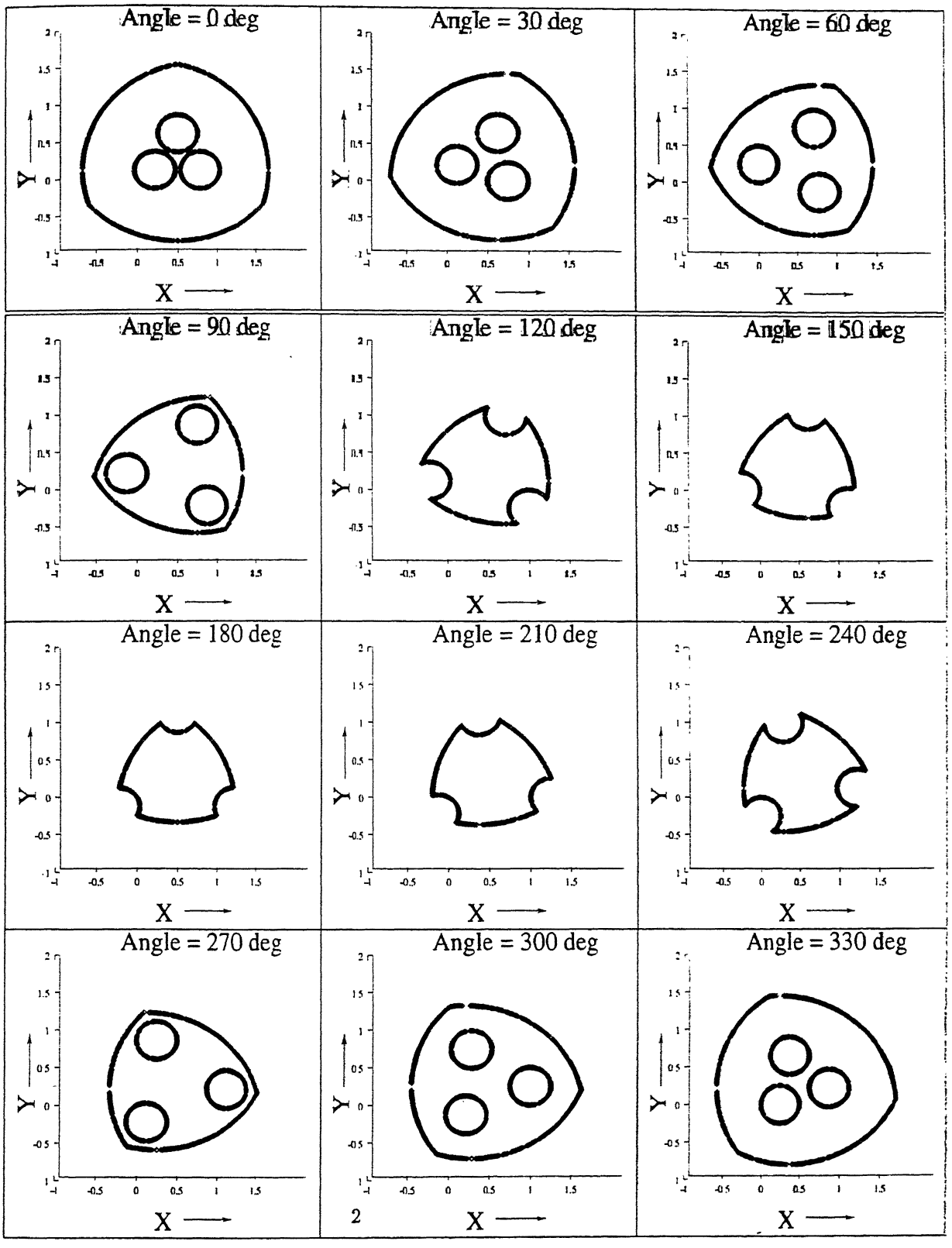

Figure 5.2: Workspace of the Prototype Manipulator with different orientations

Chapter 6

Conclusions and Suggestions for Future Work

6.1 Conclusions

This thesis addresses the design and development of 3-DOF parallel manipulator. Several topics like inverse kinematics, workspace analysis, singularity analysis of 3-DOF planar parallel manipulators are discussed. Kinematic parameters (link lengths) are calculated using optimization technique (penalty method) considering all types of singularities. Structural design of the elements of the manipulator is carried out on the basis of deflection criteria. A prototype manipulator was developed as per the dimensions obtained in design. Controller is made to control the actuators with computer. Testing of the manipulator was carried out on the basis of present work, it is observed that the manipulator achieving the desired position satisfactory.

6.2 Suggestions for Future Work

- Calibration can be done on this prototype manipulator to reduce the error in positioning. Future work include more experimentation with the prototype manipulator.
- By using motors of better resolution, the accuracy of the manipulator can be increased.
- Using Servo motors with feedback from encoders, we can position the end-effector more precisely. Homing for this manipulator can be done with suitable encoders and sensors.

- Control based on the dynamics of the prototype manipulator can be implemented further.
- By designing proper gripper mechanism, we can use this manipulator for wide variety of tasks.

Bibliography

[1] John J. Craig, "Introduction to Robotics, Mechanics and Control", Addison-Wesley Publishing Company, Inc (1986).

[2] M. Minsky, "Manipulator Design Vignettes", MIT AIL Memo 267, Cambridge, Mass. (1972).

[3] D. Stewart, "A Platform with Six Degrees of Freedom", Proc. Instn Mech. Engrs (Part I) 180(15), 371-386 (1965-66).

[4] K. H. Hunt, "Structural Kinematics of In-Parallel-Actuated Robot-Arms", Trans. ASME, J. Mech. Transm. Automn Des. 105, 705-712 (1983).

[5] G. R. Pennock and D. J. Kassner, "The Workspace of a General Geometry Planar 3-Degree-of-Freedom Platform-Type Manipulator", Trans. ASME, J. Mech. Des. 115, 269-276 (1993).

[6] O. Ma and J. Angeles, " Direct Kinematics and Dynamics of a Planar Three-DOF Parallel Manipulator", ASME DE $v32-2$, Adv. Des. Auto. Vol. 2, 313-320 (1993).

[7] C. M. Gosselin and J. P. Merlet, "The Direct Kinematics of Planar Parallel Manipulators: Special Architectures and Number of Solutions", Mech. Mach. Theory 29(8), 1083-1097 (1994).

[8] C. M. Gosselin and J. Angeles, "The Optimum Kinematic Design of a planar Three-Degree-of-Freedom Parallel Manipulator", Trans. ASME, J. Mech. Transm. Automn Des. 110, 35-41 (1988).

[9] V. Kumar, "Characterization of Workspaces of Parallel Manipulators", Trans. ASME, J. Mech. Des. 114, 368-375 (1992).

[10] V. P. Revathi, B. Dasgupta and T. S. Mruthyunjaya, "A Lagrange-Euler Formulation for the Dynamics of a Planar 3-DOF Parallel Manipulator", Proc. 7th National Conference on Machines and Mechanisms (NACOMM) 95, Durgapur, India, B1-B7 (1996).

[11] C. Gosselin and J. Angeles, "Singularity Analysis of Closed Loop Kinematic Chains", IEEE Trans. Robot. Automn 6(3), 281-290 (1990).

[12] T.Yoshikawa, "Manipulability of Robotic Mechanisms", Int. J. of Robotics Research, 4 (2), 3-9, (1985).

[13] Y. Nakamura, "Advanced Robotics: Redundancy and Optimization", Addison-Wesley Publishing Company, Inc. (1991).

[14] K. Deb, "Optimization for Engineering Design", Prentice-Hall of India, (1995).

[15] E. I. Rivin, "Mechanical Design of Robots", McGraw-Hill Book company (1988).

[16] Gerry. B. Andeen (ed), Robot Design Handbook, McGraw-Hill Book Company (1988).

[17] H. R. M. Daniali, P. J. Zsombor-Murray and J. Angeles, "Singularity Analysis of Planar Parallel Manipulators", Mech. Mach. Theory 30(5), 665-678 (1995).

[18] J. Sefrioui and C. M. Gosselin, "Singularity analysis and representation of planar parallel manipulators", Robotics and Autonomous Systems 10, 209-224 (1992).

[19] J. Sefrioui and C. M. Gosselin, "On the Quadratic Nature of the Singularity curves of Planar 3-DOF Parallel Manipulators", Mech. Mach. Theory 30(4), 533-551 (1995).

[20] B. Dasgupta, "The Stewart Platform Manipulator: Dynamic Formulation, Singularity Avoidance and Redundancy", Ph. D dissertation, Dept. Mech. Engg., IISc, Bangalore, (1996).